Electron Transfer Dynamics from Organic Adsorbate to a Semiconductor Surface: Zinc Phthalocyanine on TiO_2(110)

Daisuke Ino,[†,‡] Kazuya Watanabe,[‡,§] Noriaki Takagi,[‡,§,||] and Yoshiyasu Matsumoto*[,‡,§]

Department of Photoscience, School of Advanced Sciences, The Graduate University for Advanced Studies (Sokendai), Hayama, Kanagawa 240-0193, Japan, and National Institutes of Natural Sciences, Institute for Molecular Science, Okazaki, Aichi 444-8585, Japan

Received: April 21, 2005; In Final Form: June 28, 2005

The femtosecond time evolutions of excited states in zinc phthalocyanine (ZnPC) films and at the interface with TiO_2(110) have been studied by using time-resolved two-photon photoelectron spectroscopy (TR-2PPE). The excited states are prepared in the first singlet excited state (S_1) with excess vibrational energy. Two different films are examined: ultrathin (monolayer) and thick films of ~30 Å in thickness. The decay behavior depends on the thickness of the film. In the case of the thick film, TR-2PPE spectra are dominated by the signals from ZnPC in the film. The excited states decay with $\tau = 118$ fs mainly by intramolecular vibrational relaxation. After the excited states cascaded down to near the bottom of the S_1 manifold, they decay slowly ($\tau = 56$ ps) although the states are located at above the conduction band minimum of the bulk TiO_2. The exciton migration in the thick film is the rate-determining step for the electron transfer from the film to the bulk TiO_2. In the case of the ultrathin film, the contribution of electron transfer is more evident. The excited states decay faster than those in the thick film, because the electron transfer competes with the intramolecular relaxation processes. The electronic coupling with empty bands in the conduction band of TiO_2 plays an important role in the electron transfer. The lower limit of the electron-transfer rate was estimated to be 1/296 fs^{-1}. After the excited states relax to the states whose energy is below the conduction band minimum of TiO_2, they decay much more slowly because the electron-transfer channel is not available for these states.

1. Introduction

Electron transfer at the interfaces between organic molecules and metal or semiconductor surfaces is a fundamental process in organic semiconductor devices such as organic light emission diodes[1] and dye-sensitized photochemical cells.[2,3] In particular, ultrafast charge separation led by electron injection from electronically excited dye molecules to a conduction band of wide-gap metal oxide is a key step for improving the performance of dye-sensitized solar cells.[4] Electronic coupling strength between dye molecules and substrate is critical to the electron transfer process. In fact, strong covalent interactions of specially designed dye such as $Ru(dcbpy)_2(NCS)_2$ [(dcbpy= 4,4′-dicarboxy- 2,2′-bipyridine)] (or RuN3)[5] with TiO_2 substrate led to electron transfer in less than several tens of femtoseconds through the hybridized excited states.[6]

Numerous experiments by using femtosecond pump−probe laser spectroscopy have provided a wealth of information for an understanding of electron transfer from dye molecules to nanocrystalline TiO_2 films or TiO_2 nanoparticles.[6−9] Asbury et al.[6] reported a rising transient absorption component with $\tau = 50 \pm 25$ fs in the mid-infrared region. This fast process was assigned to the electron transfer from RuN3 dye to TiO_2 nanocrystalline thin films. One of the drawbacks in this type of measurement is that transient signals are obtained from the samples with crystallographically different surfaces where molecules are adsorbed in contrast to a single crystal surface. In addition, since transient absorption spectra only give the transition energies, it is not necessarily obvious what energy states are involved in the transitions. In addition to the real time measurements, Schnadt et al.[10] observed the resonant photoemission spectral lines of the lowest unoccupied molecular orbital (LUMO), LUMO + 1, and LUMO + 2 bands of N3 adsorbed on TiO_2(110) and estimated the lifetimes of LUMO + 1 and LUMO + 2 states to be less than 3 fs. The ultrafast electron transfer of this system is attributed to the strong covalent bonds between the carboxylate groups of RuN3 and TiO_2 surface.

To obtain a further insight into electron transfer at the interfaces between dye and semiconductor, it is essential to know the alignment of the energy levels of dye with respect to the bands of semiconductor and the energy-dependent decay dynamics of the excited states of dye homogeneously adsorbed on the surface of the semiconductor. In addition, time-resolution has to be sufficiently high to resolve ultrafast electron transfer competing with intramolecular relaxation of dye.[11−13]

Two-photon photoelectron spectroscopy has been proven to be capable of measuring the energetics of excited states of molecules adsorbed on various metal and semiconductor surfaces with submonolayer coverage.[14] Therefore, this spectroscopy with femtosecond time-resolution provides us an excellent opportunity to trace directly the relaxation process of excited states of dye in thin films and the electron transfer at the interface with semiconductor surfaces.

In this paper, we report the results of time-resolved two-photon photoelectron (TR-2PPE) spectroscopy on zinc phthalocyanine (ZnPC) adsorbed on a clean TiO_2(110) surface. Metal

* Address correspondence to this author. E-mail: matsumoto@ims.ac.jp.
[†] Current address: RIKEN, Wako, Saitama 351-0198, Japan.
[‡] The Graduate University for Advanced Studies (Sokendai).
[§] National Institutes of Natural Sciences, Institute for Molecular Science.
[||] Current Address: Department of Advanced Materials Science, University of Tokyo, Kashiwa, Chiba, 277-8561, Japan.

10.1021/jp052078d CCC: $30.25
Published on Web 09/02/2005

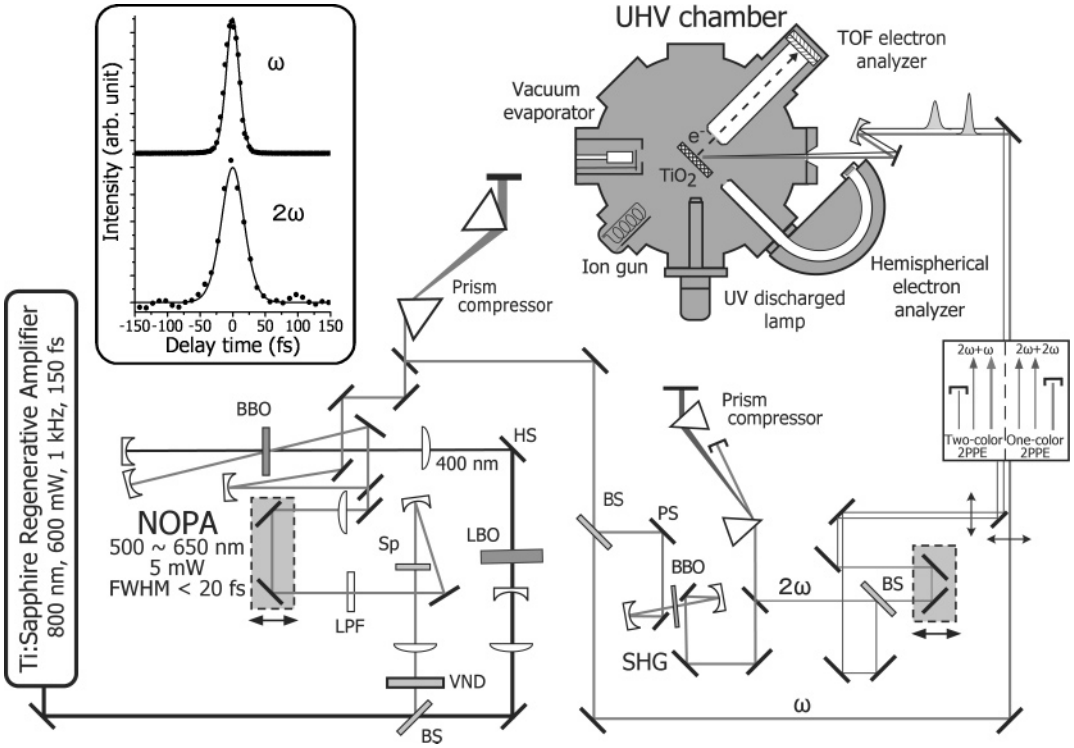

Figure 1. The experimental apparatus for fs TR-2PPE measurements: BS, beam splitter; HS, harmonic separator. In the one (two)-color 2PPE setup, 2ω (ω) + 2ω pump and probe pulses were focused on the sample. Inset: (a) autocorrelation trace of NOPA output pulses at 600 nm and (b) cross-correlation trace between NOPA output pulses and their second harmonics.

phthalocyanines have a planar structure with high symmetry. Thus, the adsorption structure and the electronic structure of phthalocyanines have been explored extensively.[15] In addition, the dye sensitization of metal oxides by using metal phthalocyanines has been also demonstrated.[16,17] Therefore, we designed the experiment by employing ZnPC adsorbed on a clean TiO_2-(110) surface as a model interface for dye-sensitizing solar cells. In this study, the intramolecular relaxation as well as electron transfer are monitored in two different films: monolayer and multilayers of ~30 Å in thickness.

2. Experimental Details

The experimental apparatus for femtosecond TR-2PPE measurements is illustrated in Figure 1. The ultrahigh vacuum (UHV) chamber (base pressure = 1.5×10^{-10} Torr) made of μ metal was equipped with a homemade time-of-flight (TOF) electron energy analyzer, a hemispherical electrostatic electron energy analyzer (VG100AX), an X-ray gun, and a He-discharged lamp. A TiO_2(110) single crystal was prereduced by annealing at 1100 K in the UHV chamber for several hours, resulting in a bluish color due to n-type carriers associated with oxygen vacancies.[18] Such reduction pins the Fermi level at near the bottom of the bulk conduction band.[18,19] The reduced TiO_2-(110) surface was cleaned by repeating cycles of Ar^+-sputtering (ion energy = 1 kV, ion current = 3 μA, 15 min), annealing at 1000 K for 15 min, and O_2-treatment at 800 K for 15 min. After the cleaning procedure, the sample was gradually cooled to room temperature in the O_2 atmosphere ($P = 1 \times 10^{-7}$ Torr).

ZnPC powder (Sigma-Aldrich, purity = 95%) was once purified by gradient sublimation in a high-vacuum chamber.[20] Purified ZnPC powder was introduced in the UHV chamber and evaporated by a homemade thermal vacuum evaporator operated in 500−550 K, and deposited to the sample surface held at 300 K. The pressure rise during ZnPC deposition was less than 3×10^{-10} Torr. The thickness of a ZnPC layer was estimated by X-ray photoelectron spectroscopy (XPS) as follows. The intensity of the O1s spectral line obtained from a ZnPC-covered surface I can be related to that from the clean surface I_0 as $I/I_0 = \exp(-d/l)$. Here, d is the thickness of the ZnPC layer and l is the electron mean free path. Since the kinetic energy of photoelectrons of the O1s line is ~700 eV when the Mg Kα resonance line is employed, we estimated l to be 21 Å from the universal curve.[21] In this study, two distinctly different ZnPC layers were used: one with $d \sim 34$ Å (hereafter denoted as thick film) and the other with $d \sim 2$ Å (ultrathin film).

A light source for femtosecond two-color TR-2PPE was a homemade double-pass noncollinear optical parametric amplification (NOPA) system (wavelength tunable from 500 to 650 nm, power = 10−15 mW, pulse width = 12 fs at 600 nm) pumped by the second harmonic output of a Ti:sapphire regenerative amplifier (Spitfire, repetition rate = 1 kHz, power = 600 mW, pulse width = 150 fs).[13] A typical pulse width of NOPA output at 536 nm was as short as 20 fs after group velocity dispersion was compensated by a fused silica prism pair. The NOPA output beam (ω) was split into two by a 50%-ultrathin beam splitter. A split beam was focused on a 60-μm thick BBO crystal to generate UV pulses (2ω) that compressed by a 45°-prism pair again. The pulse duration of UV pulses was estimated by the intensity autocorrelation of photoelectrons associated with coherent two-photon ionization of an occupied state of TiO_2(110), resulting in the full width at half-maximum (fwhm) of 35 fs at 268 nm. For one-color TR-2PPE measurements with UV pulses, laser pulses split into pump and probe pulses by a computer-controlled optical delay line. For two-color TR-2PPE measurements with visible and UV pulses, the other part of NOPA output (ω) was used for pump pulses. The pump and probe pulses were noncollinearly overlapped and focused by a spherical mirror onto the sample held in the UHV chamber. Both the pulses were p-polarized and an incident angle was 45° with respect to the surface normal.

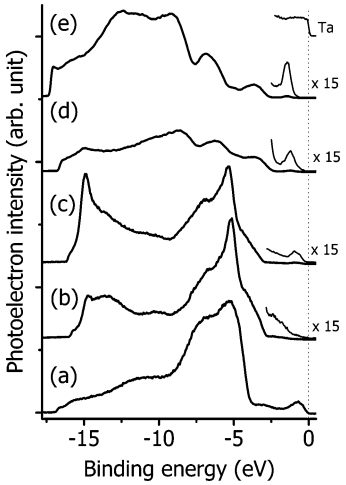

Figure 2. (a−c) HeI UPS spectra obtained from the TiO_2(110) surface during the sequential surface preparation (see the Experimental Section for details): (a) after being sputtered by Ar^+, (b) treated by O_2, and (c) briefly annealed to 1000 K. (d, e) HeI UPS spectra obtained from (d) the ultrathin- and (e) thick-ZnPC film on the TiO_2(110) surface. All the spectra were recorded along the surface normal ($\bar{\Gamma}$ point).

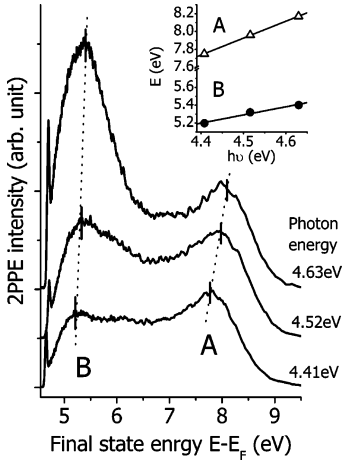

Figure 3. Photon energy dependence of one-color 2PPE spectra obtained from the clean TiO_2(110) surface. The inset shows the variation of peak energy as a function of photon energy.

The kinetic energy distributions of photoelectrons in 2PPE experiments were measured by the homemade TOF electron energy analyzer. No 2PPE signals caused by the individual pump or probe pulses were observed in the two-color 2PPE experiments when the peak power was reduced below 10 MW/cm^2. All the results of 2PPE and ultraviolet photoelectron spectroscopy (UPS) shown here were recorded along the surface normal ($\bar{\Gamma}$ point) and the sample temperature was kept at 150 K.

3. Results and Discussion

3.1. Electronic Structure of a Clean TiO_2(110) Surface. The occupied states of the clean TiO_2(110) surface were probed by HeI UPS. The UPS spectra shown in Figure 2a−c were obtained from the clean TiO_2(110) surface in the sequence of the surface cleaning process. The horizontal axis represents the binding energy E_b of electrons with respect to the Fermi level E_F of a Ta plate mounted behind the TiO_2(110) crystal. A steep rising edge originating from the valence band maximum was observed at $E_b = -2.90$ eV. In addition, the UPS measurements were used to characterize the surface stoichiometry of the clean surface. When the surface was sputtered for 15 min, a small peak appeared at $E_b = -0.69$ eV below E_F (Figure 2a). This peak disappeared after the surface was treated by O_2 for 15 min (Figure 2b). Thus, the small peak is attributed to the surface O-vacancy state lying in the bulk band gap of TiO_2.[18,22] The brief annealing of the O_2-treated surface restored the surface vacancy state appearing at $E_b = -0.93$ eV below E_F (Figure 2c). However, the intensity of the peak is smaller than that of the sputtered surface by ∼20 times. The rising edge of the valence band of the sputtered surface is shifted to higher binding energy compared with that of the O_2 treated surface. This is due to the band bending effect originating in donor-like surface defect states.[23]

Work function changes also provide some information on how the surface defects and adsorbates modify the surface potential. The work function of the sample was obtained by monitoring the cutoff of the secondary electron emission in the UP spectra. When the Ar^+-sputtered and O_2-treated surface was briefly annealed to 1000 K (Figure 2c), the work function was decreased by 0.27 eV. This is attributed to a small amount of O-vacancy site created by the annealing, which reduces the excess negative charge of oxygen extending into vacuum. When ZnPC molecules were adsorbed on this surface (Figure 2d), the work function was further decreased by 0.51 eV. This indicates that ZnPC is polarized and/or electron transfer takes place to a certain degree from the adsorbate upon adsorption.

Figure 3 shows a series of one-color 2PPE spectra obtained from the clean TiO_2(110) surface. The surface preparation procedure was the same as that employed to obtain the UPS spectrum depicted in Figure 2c. The excitation photon energy was varied from $h\nu = 4.41$ to 4.63 eV. The horizontal axis represents the final state energy of photoelectrons E with respect to E_F. There are two pronounced peaks labeled A and B in the 2PPE spectra. The excitation schemes have to be clarified for the assignment of the peaks. In the case of coherent two-photon ionization of an occupied state, E shifts twice as much as the change of photon energy ($\Delta E = 2\Delta h\nu$). On the other hand, in the case of one-photon ionization from an intermediate state populated by other photoinduced processes, E increases linearly with $h\nu$, i.e., $\Delta E = \Delta h\nu$. As shown in the inset of Figure 3, peak A shifts with a slope of $\Delta E/\Delta h\nu = 1.90 \pm 0.05$, indicating that peak A was attributed to the coherent two-photon ionization process from an occupied state. Thus, the binding energy of the occupied state is expressed as $E_b = E - 2h\nu$, resulting in $E_b = -1.02 \pm 0.05$ eV. On the other hand, peak B shifts with a slope of 0.91 ± 0.10. Thus, the intermediate excited state at $E_b = E - h\nu = 0.79 \pm 0.05$ eV is responsible for this peak.

The electronic structure emerging from the previous works[19,22,24] is useful for the assignment of the peaks observed in the 2PPE spectra. The assignment of peak A is straightforward. This peak is attributed to an occupied O-vacancy state at $E_b = -1.02$ eV, since the binding energy is in good agreement with that observed by the UPS measurements of the sample with O-vacancy sites.

On the other hand, peak B is derived from an unoccupied state above E_F. According to the theoretical investigation on the electronic structure of TiO_2(110), the contribution of the band with t_{2g} symmetry is largest among the other states in the conduction band of TiO_2.[24] Inverse photoemission spectroscopy (IPES) on clean TiO_2(110) surfaces showed the broad feature centered at ∼1 eV, which was assigned to the Ti-derived empty $2t_{2g}$ band.[19] In the current study, peak B was observed at $E_b = 0.79 \pm 0.05$ eV, whose energy is consistent with E_b of the $2t_{2g}$ band in the IPES study. Therefore, we attribute peak B to the $2t_{2g}$ band in the conduction band of TiO_2. The energy of the conduction band minimum (CBM) with respect to E_F is

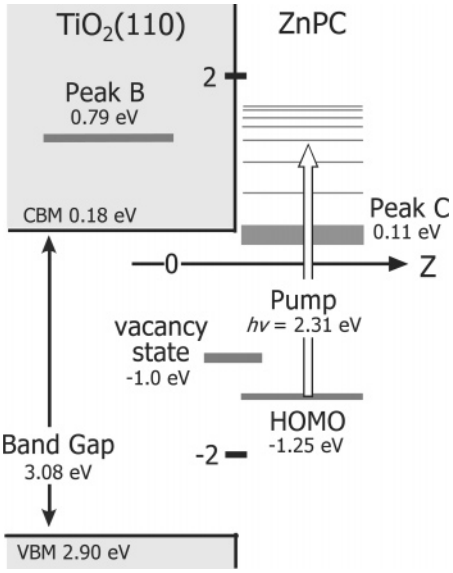

Figure 4. Energy diagram of the electronic structure of the TiO_2(110) surface covered with ZnPC.

important to obtain the proper energy alignment of adsorbate electronic states at the interface. IPES can provide this information in principle, but the precision is not enough because of its poor energy resolution and uncertainty in identifying the Fermi level.[25] We estimated the position of CBM from the leading edge of peak B, resulting in $E_b = 0.18$ eV above E_F. From this estimate together with the analysis of the UPS results, we deduced the energy of the band gap at the clean TiO_2(110) surface to be 3.08 eV at the $\bar{\Gamma}$ point. This reasonably agrees with the reported values of 3.05 eV on reduced rutile TiO_2-(110) surfaces.[26] The schematic energy diagram of the current system is presented in Figure 4.

3.2. Electronic Structure of a ZnPC-Covered TiO_2(110) Surface. The HeI UPS spectra obtained from the ZnPC-covered TiO_2(110) surface are presented in Figure 2d,e. The work function Φ of the TiO_2(110) surface decreased to 4.59 eV by the adsorption of the ultrathin (monolayer) ZnPC film. New pronounced peaks appeared in the UPS spectra at $E_b = -1.25$, -3.46, and -6.09 eV below E_F, although a small contribution from the O-vacancy states was still visible. The peak located at $E_b = -1.25$ eV was attributed to the highest occupied molecular orbital (HOMO) state of ZnPC adsorbed on the TiO_2(110) surface.[27] In the case of the ZnPC-thick film, the work function was further decreased to $\Phi = 4.01$ eV. In addition, the binding energy of the HOMO state shifted to $E_b = -1.40$ eV and its bandwidth decreased by 0.12 eV (fwhm) in comparison with the ultrathin film.

The unoccupied states of ZnPC-covered TiO_2(110) surfaces were probed by two-color 2PPE. Figure 5 shows a series of TR-2PPE spectra obtained from the ultrathin and thick ZnPC-covered TiO_2(110) surfaces. The photon energies of pump and probe pulses were $h\nu_\omega = 2.31$ and $h\nu_{2\omega} = 4.62$ eV, respectively. The 2PPE spectra were recorded as a function of pump-and-probe delay time Δt. Although both of the spectra taken from the ultrathin and thick films at $\Delta t = 0$ fs were broad and featureless, they evolve quite differently. The peak labeled C in the spectra of the thick film at $E = 4.94 \pm 0.05$ eV becomes prominent at $\Delta t = 50$ fs and persists over $\Delta t = 25$ ps, while the spectral component at $E = 5.4-5.6$ eV decayed rapidly within $\Delta t = 50$ fs.

We assigned the peak in the 2PPE spectra based on the electronic structure of vapor-deposited thin films of ZnPC

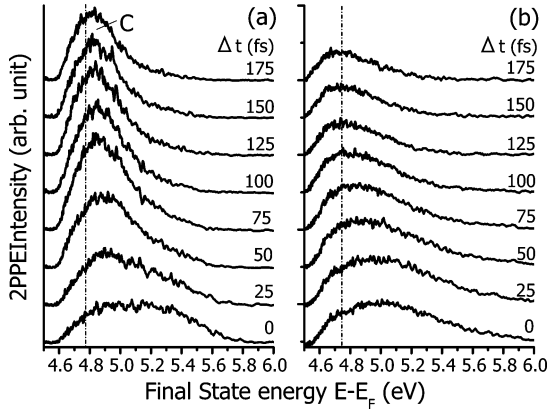

Figure 5. A series of two-color TR-2PPE spectra obtained from (a) the thick and (b) ultrathin films deposited on the TiO_2(110) surface. The photon energies of pump and probe pulses are $h\nu = 2.31$ and 4.62 eV, respectively. The vertical line at $E_b = 0.33$ eV represents the binding energy of the conduction band minimum of TiO_2(110) estimated from the 2PPE results of the clean TiO_2(110) surface.

crystallites. The absorption band corresponding to the first singlet excited-state S_1 appears at ~1.8 eV, which shows a characteristic doublet feature at 1.74 and 1.98 eV for the α form and 1.65 and 1.91 eV for the β form.[28] The spin-forbidden singlet−triplet transition was responsible for a weak absorption band in the near-IR region (1.1−1.2 eV).[15] The anion state of ZnPC thin films was observed at 3.1 eV above the HOMO state in the IPES study.[29] The current experimental results show that the energy difference between the HOMO state and the peak C is 1.73 eV, which reasonably falls in the energy range of the transition from S_0 to S_1. Therefore, we assigned the excited state responsible for peak C to the S_1 state of ZnPC adsorbed on the TiO_2(110) surface. The binding energy of the excited state was determined by $E_b = E - h\nu_{2\omega}$, resulting in $E_b = 0.33 \pm 0.03$ eV above E_F.

The 2PPE spectra obtained from the ultrathin film do not show such a pronounced peak at longer delays. The broad feature was maintained and the center of gravity of the band is shifted from $E = 4.91$ eV at $\Delta t = 50$ fs to $E = 4.73$ eV at $\Delta t = 175$ fs. The bandwidth of the peak was 0.74 eV (fwhm) at $\Delta t = 50$ fs, which is broader than that of the thick film by 0.29 eV. These features are due to the interaction with the substrate at the interface, which we discuss in detail in the next section.

3.3. Excited-State Dynamics. Excited-state dynamics of metal phthalocyanines in solutions and thin films have been extensively studied by transient absorption spectroscopy and time-resolved photoluminescence measurements. There are several relaxation pathways for the S_1 state:[30,31] (a) fluorescence decay, (b) internal conversion, (c) intersystem crossing, and (d) exciton−exciton annihilation. The fluorescence of iron tetracarboxylic phthalocyanine was observed in the solution phase, which decays with the lifetime of 1.3 ns.[32] In contrast, fluorescence quantum yields were very low in thin films owing to enhanced intersystem crossing,[33] so that the lifetime of S_1 falls in the range from a few to several tens of picoseconds. In addition to these relaxation processes, electron transfer to bulk TiO_2 also takes place in the current system.

Before we discuss the excited-state dynamics of ZnPC in detail, we comment on the electron dynamics in the conduction band of TiO_2. The one-color ($h\nu = 4.78$ eV) TR-2PPE spectra were taken from the bare TiO_2(110) surface. The autocorrelated intensity of peak B from the $2t_g$ band in the conduction band decays as fast as peak A from the occupied O-vacancy state. This indicates that the energy relaxation around $E_b = 0.18$ eV

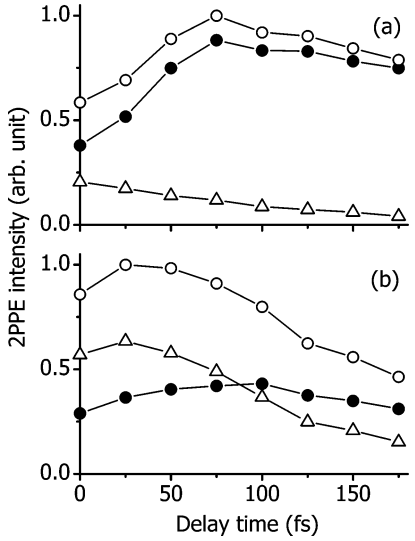

Figure 6. Photoelectron yields in the 2PPE spectra as a function of pump-and-probe delay. (a) Thick film: the yields are obtained by integrating the intensity of 2PPE signals in the entire energy range (total yield, open circle), in $4.55 < E < 5.1$ eV (solid circle) and in $E \geq 5.1$ eV (open triangle). (b) Ultrathin film: the yields are obtained by integrating the intensity of 2PPE signals in the entire energy range (total yield, open circle), in $4.5 < E < 4.8$ eV (solid circle) and in $E \geq 4.8$ eV (open triangle).

in the conduction band takes place very rapidly, i.e., within the laser pulse duration of 35 fs.

Now we discuss the excited-state dynamics in the thick film. As noted in Figure 5, peak C grows with the increase of delay in the TR-2PPE spectra. To examine more explicitly how the excited states in high and low energy ranges evolve differently, we plot the integrated yields of photoelectrons above and below $E = 5.1$ eV in Figure 6a. The total photoelectron yield increases until $\Delta t \sim 70$ fs and the yield below $E = 5.1$ eV follows this trend. As we describe later, the excited states in the energy range have a long lifetime of $\tau \sim 60$ ps. Thus, the apparent rising signals of $E < 5.1$ eV are mostly due to the slow response of the system. On the other hand, the excited states above $E = 5.1$ eV have a short lifetime, so that the photoelectron yield in the higher energy range does not show such a rising component and decays exponentially with $\tau = 118$ fs.

More details of the time evolution around peak C are given by cross-correlation measurements depicted in Figure 7a. The trace was fitted with

$$I(\Delta t) = \sum_{i=1,2} A_i \int_{-\infty}^{\infty} \mathrm{d}t \int_{-\infty}^{t} \mathrm{d}T\, f(T) \exp\left(-\frac{t-T}{\tau_i}\right) g(t-\Delta t) + B\int_{-\infty}^{\infty} \mathrm{d}t f(t)\, g(t-\Delta t) \quad (1)$$

Here, τ_i is the lifetime of a decay component and $f(t)$ and $g(t)$ are the pulse-shape functions of pump and probe pulses, respectively. A cross-correlation trace of 2PPE signals from the occupied O-vacancy state of the clean TiO_2(110) surface was used for determining the laser pulse shape. The first term represents the contributions of two exponentially decaying functions convoluted with the laser pulses, originating from a sequential two-photon excitation process. The second term is the contribution of coherent artifact arising from a coherent 2PPE process from an occupied state. The fitting parameters obtained are listed in Table 1. The slowly decaying component at peak C is more evident in the cross-correlation trace. The trace is composed of the fast and the slow decay components with $\tau_1 = 140 \pm 12$ fs and $\tau_2 = 56.2 \pm 0.5$ ps, respectively.

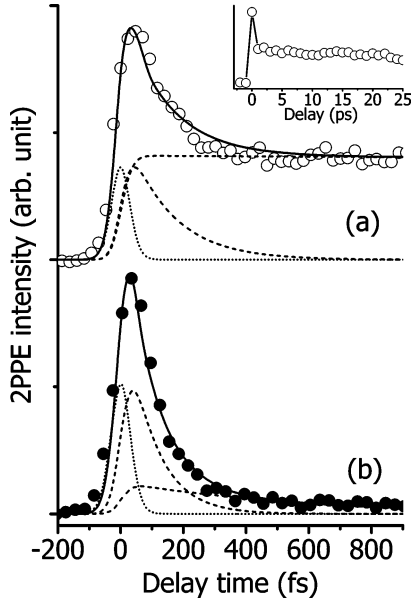

Figure 7. Cross-correlation traces of 2PPE signals originating from the S_1 state of ZnPC in (a) the thick and (b) the ultrathin films. The 2PPE intensity with the final state energy from 4.65 (4.75) to 5.00 (5.10) eV was recorded as a function of Δt for the ultrathin (thick) film. Dotted lines are exponential decay functions convoluted with the pulse-shape function of pump pulses, and dashed lines are the cross-correlation trace between the pump and probe pulses. The inset shows the cross-correlation trace up to 25 ps.

TABLE 1: Fitting Parameters of Eq 1 for the Cross-Correlation Traces of the S_1 State

d (Å)	A_1	A_2	τ_1 (fs)	τ_2 (ps)
2	0.57	0.12	95 ± 8	0.6 ± 0.1
34	0.41	0.45	140 ± 12	56.2 ± 0.5

From these results, the excited-state dynamics in the thick film is characterized by at least three decaying components: $\tau = 118$ fs at $E > 5.1$ eV and 140 fs and 56 ps at $E \sim 4.8$ eV, i.e., around peak C. All the decaying components are not due to electrons in the conduction band transferred from the ZnPC film, because the energy relaxation of electrons in the energy range of the conduction band decays much faster as noted earlier. In addition, since the molecules at the interface would be less than 10% of the entire molecules in the thick film, the 2PPE signals are rather dominated by molecules inside the film instead of ones at the interface. Thus, those decaying components are mostly associated with the intramolecular relaxation processes of the excited states of molecules in the thick film.

Since the photon energy of the pump pulse exceeds the absorption maximum of the $S_0 \rightarrow S_1$ transition by 0.6 eV,[34] ZnPC molecules are excited to vibrationally excited states in the S_1 manifold. At this energy, the absorption cross section is less than that at the peak of the $S_0 \rightarrow S_1$ transition by 1 order of magnitude.[34] Furthermore, the excitation power in the experiments was less than 10 MW/cm^2. This is much smaller than that used for the measurements where exciton−exciton annihilation was observed. Thus, the exciton−exciton annihilation would be ruled out in the current measurements. Consequently, we assign the fast component with $\tau = 118$ fs in $E > 5.1$ eV to the intramolecular vibrational relaxation of highly vibrationally excited states in the S_1 manifold. Since the photoelectrons at $E \sim 4.8$ eV stem from the electronic states at near the bottom of the S_1 manifold, little excess vibrational energy is left. Thus, the decay component with $\tau = 140$ fs at $E \sim 4.8$ eV is due to the internal conversion to the ground state. The longer time constant of $\tau = 56$ ps at $E \sim 4.8$ eV reasonably

falls in the range of the S_1-state lifetime in ZnPC films measured in the past. Thus, the slow decay component was attributed to the transition to the triplet state via enhanced intersystem crossing.

In the case of the ultrathin film the TR-2PPE spectrum evolves very differently compared to the thick film. The difference in the decay behavior is evident in the cross-correlation result shown in Figure 7b. The cross-correlation trace measured at $E = 4.65-5.0$ eV contains two decay components with $\tau_1 = 95 \pm 8$ and $\tau_2 = 577 \pm 107$ fs. These decaying components also originate from electrons in the thin film and not from ones transferred in the conduction band, since the decay rates are much longer than that of electrons in the conduction band. However, the decaying component with $\tau_1 = 95$ fs faster than that of the thick film at this range of excess energy ($\tau = 140$ fs) indicates the opening of a new channel, i.e., electron transfer to the bulk TiO_2, because the molecules in the ultrathin film interact with the surface directly. If the intramolecular relaxation takes place with the similar rate as in the case of the thick film, the total decay rate k_t is the sum of the rate of intramolecular relaxation k_i and that of the electron-transfer process k_{et}. By using $k_t = 1/95$ fs^{-1} and $k_i = 1/140$ fs^{-1}, we estimate $k_{et} = 1/296$ fs^{-1}. Since the electron transfer may also partly contribute to the fast decaying component of the thick film, the electron-transfer rate estimated here provides its lower limit.

The contribution of electron transfer in the ultrathin film is more evident if we plot photoelectron yields as a function of pump−probe delay as shown in Figure 6b. In addition to the total yield, the yields above and below the energy of the CBM of TiO_2 are also plotted. In contrast to the case of the thick film, the total yield decreases significantly by $\Delta t = 175$ fs owing to electron transfer to the substrate. The photoelectron yield above CBM basically follows the trend of the total yield and decays fast with $\tau = 94 \pm 7$ fs. On the other hand, the yield below CBM is almost constant and decays slowly. This indicates that the vibronic states above CBM decay fast due to electron transfer in addition to intramolecular relaxation processes, while those below CBM have a long lifetime, since the electron-transfer channel is closed and the vibrational relaxation is almost quenched at the bottom of the first singlet excited state.

The electronic coupling strength between donor and acceptor is one of the critical factors to electron transfer. The electron-transfer rate estimated in this study is slower than those estimated at the interfaces with RuN3,[10] alizarin,[35] and hydrated OH[36] by almost 2 orders of magnitude. These adsorbates showing extremely fast electron injection rates are all covalently bonded to TiO_2 surfaces, i.e., the electronic coupling is very strong. As shown in the studies with scanning tunneling microscopy on various metal phthalocyanines,[37−39] ZnPC likely lies flat on the surface. Thus, the LUMO of ZnPC ($7e_g$) with π symmetry[40] has the right symmetry with the $2t_{2g}$ state of TiO_2-(110) in this adsorption structure. However, the lack of direct coupling between the chromophore and surface atoms in the current system results in the slower injection rate. Even if adsorbate is anchored by covalent bonding to semiconductor surfaces, the characteristic times for electron transfer become longer and fall in the range of ten to a few hundred femtoseconds when a molecular spacer group with saturated bonds is inserted between the chromophore and the surface atoms.[41]

As described earlier, although electrons transferred from the excited states of dye molecules to the conduction band of TiO_2 decay very rapidly in the conduction band, electrons near the CBM decay with the lifetime of several hundreds of picoseconds.[6,7,42] This is because electron−hole recombination in the bulk takes place slowly. Such a long decaying component is difficult to observe in this study, since the lifetime in the range of several hundreds of picosecond was too long to observe by TR-2PPE spectroscopy with relatively short delays used in the current measurements.

4. Conclusion

We investigated the electronic structure and the ultrafast electron relaxation dynamics of ZnPC thin films and at the interface with TiO_2(110) by UPS and TR-2PPE. The direct observation for the time evolution of 2PPE spectra clarifies both the electron transfer at the interface and the excited-state dynamics in the ZnPC films. In the thick film, the excited states with excess vibrational energy decays to the bottom of the S_1 state rapidly ($\tau = 118$ fs) by intramolecular vibrational relaxation, and decays more slowly ($\tau = 50$ ps) by intersystem crossing to the triplet state. Electron transfer from the thick film to the bulk TiO_2 should occur, but is not evident in the TR-2PPE spectra.

In contrast, electron transfer to the bulk TiO_2 is evident in the case of the ultrathin film. When the excited states are located at above the CBM of bulk TiO_2, they decay with $\tau = 95$ fs even at near the bottom of the S_1 state, indicating that the electron transfer competes with the internal conversion. In the electron-transfer process the electronic coupling between LUMO-($7e_g$) of ZnPC and the $2t_{2g}$-states in the conduction band of TiO_2 plays an important role. The excited states below CBM of TiO_2 decay much more slowly, since the electron-transfer channel is closed for these states.

Acknowledgment. This work was supported in part by Grants-in-Aid for Young Scientists (A)(14703009), Scientific Research on Priority Area (417), and Creative Scientific Research Collaboratory on Electron Correlation-Toward a New Research Network between Physics and Chemistry (13NP0201) from the Ministry of Education, Culture, Sports, Science and Technology (MEXT) of Japan, and KAKENHI (17105001) from the Japan Society for the Promotion of Science (JSPS).

References and Notes

(1) Tang, C.; VanSlyke, S. *Appl. Phys. Lett.* **1987**, *51*, 913.
(2) O'Regan, B.; Grätzel, M. *Nature* **1991**, *353*, 737.
(3) Grätzel, M. *Nature* **2001**, *414*, 338.
(4) Rehm, J. M.; McLendon, G. L.; Nagasawa, Y.; Yoshihara, K.; Moser, J.; Grätzel, M. *J. Phys. Chem.* **1996**, *100*, 9577.
(5) Nazeeruddin, M. K.; Kay, A.; Rodicio, I.; Humphry-Baker, R.; Müller, E.; Liska, P.; Vlachopoulos, N.; Grätzel, M. *J. Am. Chem. Soc.* **1993**, *115*, 6382.
(6) Asbury, J. B.; Hao, E.; Wang, Y.; Ghosh, H. N.; Lian, T. *J. Phys. Chem. B* **2001**, *105*, 4545.
(7) Hilgendorff, M.; Sundström, V. *Chem. Phys. Lett.* **1998**, *287*, 709.
(8) Asbury, J. B.; Hirendra, R. J.; Ghosh, N.; Ferrere, S.; Nozik, A. J.; Lian, T. *J. Phys. Chem.* **1999**, *103*, 3110.
(9) Katoh, R.; Furube, A.; Kohjiro, K.; Murata, S.; Sugiara, H.; Arakawa, H.; Tachiya, M. *J. Chem. Phys.* **2002**, *106*, 12957.
(10) Schnadt, J.; Brühwiler, P. A.; Patthey, L.; O'Shea, J. N.; Södergren, S.; Odelius, M.; Ahuja, R.; Karis, O.; Bässler, M.; Persson, P.; Siegbahn, H.; Lunell, S.; Måtensson, N. *Nature* **2002**, *418*, 620.
(11) Yeh, A. T.; Shank, C. V.; McCusker, J. K. *Science* **2000**, *289*, 935.
(12) Ge, N. H.; Wong, C. M.; Lingle, R. L., Jr.; Mcneill, J. D.; Gaffney, K. J.; Harris, C. B. *Science* **1998**, *279*, 202.
(13) Ino, D.; Watanabe, K.; Takagi, N.; Matsumoto, Y. *Chem. Phys. Lett.* **2004**, *383*, 261.
(14) Steinman, W.; Fauster, T. *Laser spectroscopy and photochemistry on metal surfaces, Part 1*; World Scientific: Singapore, 1995.
(15) Wöhrle, D. L. K.; Schlettwein, D. *Phthalocyanines—Properties and Applications*; Verlag Chemie: New York, 1996.
(16) Jaeger, C. D.; Fan, F. F.; Bard, A. J. *J. Am. Chem. Soc.* **1980**, *102*, 2592.

(17) Yanagi, H.; Chen, S.; Lee, P. A.; Nebesny, K. W.; Armstrong, N. R.; Fujishima, A. *J. Phys. Chem.* **1996**, *100*, 5447.
(18) Henrich, V. E.; Dresselhaus, G.; Zeiger, H. *Solid State Phys.* **1976**, *36*, 1335.
(19) See, A. K.; Bartynski, R. A. *Phys. Rev. B* **1994**, *50*, 12064.
(20) Forrest, S. R. *Chem. Rev.* **1997**, *97*, 1793.
(21) Seah, M. P.; Dench, W. A. *Surf. Interface Anal.* **1979**, *1*, 2.
(22) Onda, K.; Li, B.; Petek, H. *Phys. Rev. B* **2004**, *70*, 045415.
(23) Diebold, U. *Surf. Sci. Rep.* **2003**, *48*, 53.
(24) Munnix, S.; Schmeits, M. *Phys. Rev. B* **1984**, *30*, 2202.
(25) Yang, S.; Garrison, K.; Bartynski, R. A. *Phys. Rev. B* **1991**, *43*, 2025.
(26) Tang, H.; Lévy, F.; Berger, H.; Schmid, P. E. *Phys. Rev. B* **1995**, *52*, 7771.
(27) Schlettwein, D.; Armstrong, N. R. *J. Phys. Chem.* **1994**, *98*, 11771.
(28) Lucia, E. A.; Verderame, F. D. *J. Chem. Phys.* **1968**, *48*, 2674.
(29) Gao, W.; Kahn, A. *Org. Electron.* **2002**, *3*, 53.
(30) Gulbinas, V.; Chachisvilis, M.; Valkunas, L.; Sundström, V. *J. Phys. Chem.* **1996**, *100*, 2213.
(31) Terasaki, A.; Hosoda, M.; Wada, T.; Tada, H.; Koma, A.; Yamada, A.; Sasabe, H.; Garito, A. F.; Kobayashi, T. *J. Phys. Chem.* **1992**, *96*, 10534.
(32) Ma, G.; He, J.; Kang, C.-H.; Tang, S.-H. *Chem. Phys. Lett.* **2003**, *370*, 293.
(33) Sakakibara, Y.; Bera, R. N.; Mizutani, T.; Ishida, K.; Tokumoto, M.; Tani, T. *J. Phys. Chem. B* **2001**, *105*, 1547.
(34) Wróbel, D.; Boguta, A. *J. Photochem. Photobiol. A* **2002**, *150*, 67.
(35) Huber, R.; Moser, J.-E.; Gra1tzel, M.; Wachtveitl, J. *J. Phys. Chem. B* **2002**, *106*, 6494.
(36) Onda, K.; Li, B.; Zhao, J.; Jordan, K. D.; Yang, J.; Petek, H. *Science* **2005**, *308*, 1154.
(37) Hipps, K. W.; Lu, X.; Wang, D.; Mazur, U. *J. Phys. Chem.* **1996**, *100*, 11207.
(38) Lu, X.; Hipps, K. W. *J. Phys. Chem. B* **1997**, *101*, 5391.
(39) Qiu, X. H.; Nazin, G. V.; Ho, W. *Phys. Rev. Lett.* **2004**, *92*, 206102.
(40) Nguyen, K. A.; Pacher, R. *J. Chem. Phys* **2001**, *114*, 10757.
(41) Zimmermann, C.; Willig, F.; Ramakrishna, S.; Burfeindt, B.; Pettinger, B.; Eichberger, R.; Storck, W. *J. Phys. Chem. B* **2001**, *105*, 9245.
(42) Burfeindt, B.; Hannappel, T.; Storck, W.; Willig, F. *J. Phys. Chem.* **1996**, *100*, 16463.